A carboxylated Zn-phthalocyanine inhibits fibril formation of Alzheimer's amyloid β peptide

Shatera Tabassum[1], Abdullah Md. Sheikh[1], Shozo Yano[1], Takafumi Ikeue[2], Makoto Handa[2], Atsushi Nagai[1]*

[1]Department of Laboratory Medicine, Shimane University School of Medicine, 89-1 Enya Cho, Izumo 693-8501, Japan

[2]Department of Material Science, Interdisciplinary Faculty of Science and Engineering, Shimane University, 1060 Nishikawatsu, Matsue 690-8504, Japan

Running title: ZnPc inhibits Aβ fibril formation

*Address correspondence to:

Atsushi Nagai

Department of Laboratory Medicine

Shimane University School of Medicine

89-1 Enya Cho, Izumo 693-8501,

Japan

Tel.: +81-0853-20 2312

Fax: +81-0853-20 2312

E mail anagai@med.shimane-u.ac.jp

Key words: amyloid β, phthalocyanine, Alzheimer's disease, fibril formation, near infrared.

Abstract:

Amyloid β (Aβ), a 39- to 42-amino-acid peptide derived from amyloid precursor protein, is deposited as fibrils in Alzheimer's disease (AD) brains and is considered to have a major role in the pathogenesis of the disease. We have investigated the effects of a water-soluble Zn-phthalocyanine, $ZnPc(COONa)_8$, a macrocyclic compound having near-infrared optical properties, on Aβ fibril formation *in vitro*. Thioflavin T (ThT) fluorescence assay demonstrated that $ZnPc(COONa)_8$ significantly inhibited Aβ fibril formation, increasing the lag time and dose-dependently decreasing the plateau level of fibril formation. Moreover, it destabilized pre-formed Aβ fibrils, resulting in an increase of low-molecular-weight species. After fibril formation in the presence of $ZnPc(COONa)_8$, immunoprecipitation of $Aβ_{1-42}$ with Aβ-specific antibody followed by near-infrared scanning demonstrated binding of $ZnPc(COONa)_8$ to $Aβ_{1-42}$. ANS study demonstrated that $ZnPc(COONa)_8$ decreased the hydrophobicity during $Aβ_{1-42}$ fibril formation. CD spectroscopy showed an increase of α helix and a decrease of β sheet structure of $Aβ_{1-40}$ in fibril-forming buffer containing $ZnPc(COONa)_8$. SDS-PAGE and dot blot immunoassay demonstrated that $ZnPc(COONa)_8$ delayed the disappearance of low-molecular-weight species and

the appearance of higher-molecular-weight oligomeric species of $A\beta_{1-42}$. Cell viability assay (MTT assay) showed that $ZnPc(COONa)_8$ was not toxic to neuronal cell line (A1), rather protected A1 cells against $A\beta_{1-42}$-induced toxicity. Overall, our results indicate that $ZnPc(COONa)_8$ binds to Aβ and decreases the hydrophobicity, and this change is unfavorable for Aβ oligomerization and fibril formation.

Introduction:

Alzheimer's disease (AD) is a common dementia of the elderly [1]. It is characterized pathologically by degeneration of neurons, mainly of cholinergic type, in the hippocampal and cortical areas [2,3]. Histologically, dystrophic neurons and reactive glial cells are found in those areas, concomitantly with extracellular deposition of amyloid β (Aβ) peptide and intracellular formation of neurofibrillary tangles [2]. A large body of evidence suggests that Aβ peptide has a critical role in the pathogenesis of AD. For example, gene mutations that affect the production or processing of Aβ precursor protein and increase the peptide burden are related to AD lesion formation and progression of the disease [4- 10]. Increased Aβ peptide burden leads to aggregation, affording oligomers or polymeric fibrils that are deposited in the brain parenchyma [6]. Aggregated forms, especially Aβ oligomers, are more neurotoxic than the monomers in vitro [11, 12], suggesting that Aβ accumulation and aggregation play key roles in the disease pathogenesis. Hence, these processes might be good targets for diagnosis and therapy of AD.

Recent research on the pathophysiology of AD has suggested that inhibitors of Aβ accumulation and aggregation, or enhancers of fibril degradation, would be candidates for therapy of the disease. Several compounds that show anti-amyloid activity *in vitro* or in animal models are already in clinical trials [13, 14]. However, an effective disease-modifying therapy remains elusive.

Diagnosis is also an important issue, and several groups are examining the usefulness of Aβ peptide in CSF or deposited in brain parenchyma as a diagnostic marker [15, 16]. Deposited Aβ can be visualized by PET imaging, but

the equipment is expensive and not widely available [16]. On the other hand, near-infrared (NIR) spectroscopy is technically favorable for in vivo imaging, because there is an optical window from approximately 600 to 1000 nm where the absorption coefficient of tissue is at a minimum, resulting in a low background [17]. NIR has higher tissue penetration capability than visible light [17]. Recently, it was reported that phthalocyanines, which are metal-containing, aromatic, macrocyclic NIR fluorophores, interact with α-synuclein and affect fibril formation [18]. Further, iron-containing phthalocyanine interacts with toxic $A\beta_{1-40}$ oligomers and converts them to an amyloid fibril meshwork [19]. Thus, we hypothesized that phthalocyanines might bind to Aβ and serve as amyloid fibril-modifying agents. If this is the case, they might have therapeutic potential for AD. They might also be useful as amyloid-specific NIR imaging probes to visualize deposited Aβ peptide in AD brains *in vivo*.

Most phthalocyanine species are hydrophobic, and tend to aggregate in aqueous medium, resulting a self-quenching effect on their excited state [20, 21]. Therefore, we prepared water-soluble Zn-containing phthalocyanines (ZnPc) bearing sodium carboxylate groups as candidate amyloid fibril-modifying agents or *in vivo* NIR probes. The chemical structures of the four phthalocyanines used in this study are shown in figure 1. Among them, carboxylated ZnPc was found to bind with Aβ peptide and to inhibit Aβ aggregation and neurotoxicity.

Results:

Interactions of phthalocyanines with $A\beta_{1-40}$ and $A\beta_{1-42}$ and effect on fibril

formation. Initially, $A\beta_{1-40}$ (50 μM) and $A\beta_{1-42}$ (12.5 μM) were each incubated with increasing concentrations of $ZnPc(COONa)_8$, $ZnPc(COONa)_{16}$, $ZnPc(COOC_5H_{11})_8$ and PdPc dimer in fibril-forming buffer for 48 h or 24 h. Evaluation of fibril formation by thioflavin T (ThT) fluorescence assay revealed that $ZnPc(COONa)_8$ efficiently and dose-dependently inhibited fibril formation of both $A\beta_{1-40}$ and $A\beta_{1-42}$ (figure 2A and 2B). The effect was more pronounced in the case of $A\beta_{1-40}$ (compare figure 2A and 2B). $ZnPc(COONa)_{16}$ also modestly inhibited $A\beta_{1-40}$ and $A\beta_{1-42}$ fibril formation at higher concentrations (figure 2C and 2D). PdPc dimer inhibited only $A\beta_{1-40}$ fibril formation at relatively high concentrations (figure 2G and 2H). On the other hand, $ZnPc(COOC_5H_{11})_8$ significantly and dose-dependently increased fibril formation of $A\beta_{1-40}$, but not $A\beta_{1-42}$ (figure 2E and 2F).

Effects of $ZnPc(COONa)_8$ on fibril formation kinetics of $A\beta_{1-40}$ and $A\beta_{1-42}$. In order to investigate the fibril formation kinetics, $A\beta_{1-40}$ (50 μM) or $A\beta_{1-42}$ (12.5 μM) was incubated in the absence or presence of 5 μM $ZnPc(COONa)_8$. Fibril formation of both $A\beta_{1-40}$ and $A\beta_{1-42}$ showed sigmoid kinetics, with lag times of about 12 h and 8 h, respectively (figure 3A and 3B). Once fibril formation started, it increased exponentially, reaching a plateau at 48 h for $A\beta_{1-40}$, and 24 h for

$A\beta_{1-42}$ (figure 3A and 3B). $ZnPc(COONa)_8$ extended the lag time to 24 h and the plateau time to 72 h for $A\beta_{1-40}$ (figure 3C). For $A\beta_{1-42}$, the lag time was slightly increased to between 8 and 16 h, while the plateau time showed little change (figure 3D). $ZnPc(COONa)_8$ significantly decreased the plateau fluorescence levels of both $A\beta_{1-40}$ ($A\beta_{1-40}$=57±8.3 vs $A\beta_{1-40}$+$ZnPc(COONa)_8$=12.3±2.4) and $A\beta_{1-42}$ ($A\beta_{1-42}$=20.1±0.8 vs $A\beta_{1-42}$+$ZnPc(COONa)_8$=4.5±0.4).

Next, the morphology of Aβ fibrils was evaluated by transmission electron microscopy. $ZnPc(COONa)_8$ had no apparent effect on the morphology of $A\beta_{1-40}$ or $A\beta_{1-42}$ fibrils (figure 3E).

In this study, ThT fluorescence assay was mainly employed for quantitative analysis of Aβ fibrils. However, the presence of $ZnPc(COONa)_8$ could influence ThT fluorescence [22]. Therefore, to confirm the inhibitory effect, fibrils were removed from the samples by filtration after fibril formation of $A\beta_{1-42}$ (100 μM) in the absence or presence of $ZnPc(COONa)_8$ (5 μM) for 24 h. The filtrate contained only non-fibrillar $A\beta_{1-42}$, as revealed by ThT fluorescence assay. The protein concentration of the filtrate was measured, and was 235 ± 8.2% higher in the $A\beta_{1-42}$ sample containing $ZnPc(COONa)_8$, compared to the $A\beta_{1-42}$ alone condition (figure 3F). This result supports the idea that $ZnPc(COONa)_8$

inhibits fibril formation.

Effect of $ZnPc(COONa)_8$ on the stability of Aβ fibrils. Next, the effect of $ZnPc(COONa)_8$ on the stability of Aβ fibrils was investigated. Increasing concentrations of $ZnPc(COONa)_8$ were added to preformed $Aβ_{1-40}$ and $Aβ_{1-42}$ fibrils, and the mixtures were incubated for 24 h. ThT fluorescence assay showed that $ZnPc(COONa)_8$ dose-dependently decreased both $Aβ_{1-40}$ and $Aβ_{1-42}$ fibril levels at the end of the incubation period (figure 4A and 4B). Moreover, SDS PAGE confirmed that $ZnPc(COONa)_8$ increased the levels of low-molecular-weight species of $Aβ_{1-40}$ and $Aβ_{1-42}$, at least at high concentrations (figure 4C and 4D).

Effects of sodium azide on Aβ fibril formation. Phthalocyanines are reported to produce singlet oxygen [23]. Therefore, we investigated whether singlet oxygen is responsible for the inhibitory effect of $ZnPc(COONa)_8$ by using sodium azide (NaN_3) as a singlet oxygen scavenger [24]. We first confirmed that NaN_3 alone (up to 50 mM) had no effect on $Aβ_{1-40}$ and $Aβ_{1-42}$ fibril formation (figure 5A and 5B). Next, increasing concentrations of NaN_3 (up to 50 mM) were incubated with $Aβ_{1-40}$ and $Aβ_{1-42}$ in the presence of $ZnPc(COONa)_8$. ThT fluorescence assay indicated that NaN_3 had no effect on $ZnPc(COONa)_8$-mediated inhibition

of $A\beta_{1-40}$ and $A\beta_{1-42}$ fibril formation (figure 5C and 5D).

Binding of $ZnPc(COONa)_8$ to $A\beta_{1-42}$ peptide. Next, we investigated whether $ZnPc(COONa)_8$ directly binds to Aβ peptide by adding increasing concentrations of $ZnPc(COONa)_8$ to $A\beta_{1-42}$ monomers or pre-formed fibrils. After incubation for 24 h in a fibril-forming environment, $A\beta_{1-42}$ was immunoprecipitated with Aβ-specific antibody, and $ZnPc(COONa)_8$ in the immunoprecipitate was quantitated by near-infrared scanning. In the case of $A\beta_{1-42}$ monomer, the near-infrared signal of $ZnPc(COONa)_8$ in the immunoprecipitates increased linearly with increasing concentration of the compound (figure 6A). A similar effect was observed with pre-formed $A\beta_{1-42}$ fibrils, though the signal intensities were much lower than with $A\beta_{1-42}$ monomer (figure 6A).

Effect of ZnPc on the microenvironment of fibril formation. To further explore the mechanism of the inhibition, we investigated whether binding of $ZnPc(COONa)_8$ alters the microenvironment of Aβ fibril formation. Hydrophobic amino acids in Aβ peptide, as well as a hydrophobic microenvironment, play a key role in fibril formation (25-27). We used 8-anilino-1-naphthalenesulfonic acid (ANS) as a hydrophobic fluorescent probe; its fluorescence in aqueous solution is minimal, but upon binding to nonpolar amino acids, the fluorescence

increases and shows a blue shift [28]. Hence, ANS is useful to analyze conformational changes of proteins or peptides in solution. We found that incubation of $A\beta_{1-42}$ in fibril-forming buffer for 4 h caused an increase of the fluorescence intensity, together with a blue shift (figure 6B, 6C and 6D). But, when $ZnPc(COONa)_8$ was added to the buffer, the intensity was decreased significantly and the peak showed a red shift compared to the $A\beta_{1-42}$-only counterpart (figure 6B, 6C and 6D).

Effect of $ZnPc(COONa)_8$ on the secondary structures and molecular species of Aβ peptide. Hydrophobic interaction is important in secondary structure formation and aggregation of Aβ peptides [25, 29, 30]. As $ZnPc(COONa)_8$ decreased the hydrophobicity of Aβ, we investigated whether it influenced the secondary structures of the peptide. $ZnPc(COONa)_8$ (2 μM) was added to $A\beta_{1-40}$ (100 μM) monomer in a fibril-forming buffer, and the mixture was incubated at 37°C for 0 and 2 h, then diluted with water to make final concentrations of $A\beta_{1-40}$ and $ZnPc(COONa)_8$ of 10 μM and 0.2 μM, respectively. Representative CD spectra of $A\beta_{1-40}$ in the presence or absence of $ZnPc(COONa)_8$, after 0 and 2 h incubation are shown in figure 7A. The CD spectra (figure 7B) indicated that in fibril formation buffer, about 37.2±7.6% of the

peptide adopted β sheet structure, whereas only 5±2.3% showed α helix structure. After 2 h incubation, the percentage of α helix showed little change (3.7±1.5%), but β sheet was increased to 48.6 ± 0.2%. When $ZnPc(COONa)_8$ was added to the fibril-forming buffer, 18.7 ± 0.9% of the peptide exhibited α helix structure, whereas β sheet amounted to only 4.9 ± 3%. After 2 h incubation, the percentages of α helix and β sheet were 17.6 ± 3.5 and 17.2 ± 5.9, respectively.

Next, after fibril formation in the absence or presence of $ZnPc(COONa)_8$, the peptide was subjected to SDS-PAGE and Aβ species were visualized by Coomassie Blue staining. $Aβ_{1-42}$ was detected mainly as monomer, dimer and trimer. Dimer and trimer started to decrease after 1 h incubation, and monomer was decreased from 2 h. $ZnPc(COONa)_8$ inhibited the time-dependent decrease of these low-molecular-weight $Aβ_{1-42}$ species at 1, 2 and 4 h (figure 7C).

Then, the effect of $ZnPc(COONa)_8$ on $Aβ_{1-42}$ oligomers was investigated. Dot blot immunoassay using an oligomer-specific antibody demonstrated that $Aβ_{1-42}$ oligomers were detectable after 4 h incubation (figure 7D). $ZnPc(COONa)_8$ delayed the appearance time of $Aβ_{1-42}$ oligomers to 8 h (figure 7D).

Effect of ZnPc(COONa)$_8$ on Aβ$_{1-42}$-induced cytotoxicity. Oligomers of Aβ peptides are considered to be more cytotoxic than the monomers [11, 12]. As ZnPc(COONa)$_8$ inhibited oligomer formation, we explored whether it affected Aβ$_{1-42}$-induced cytotoxicity to a neuronal cell line (A1). Morphological study of cultured A1 cells showed that increasing concentrations of Aβ$_{1-42}$ decreased the cell density, and the cell body became round and smaller in size (figure 8A). ZnPc(COONa)$_8$ alone did not alter the density or morphology of the cultured cells (figure 8A). Interestingly, addition of ZnPc(COONa)$_8$ to the culture partially rescued the cells from Aβ$_{1-42}$-induced reduction of cell density and morphological change (figure 8B).

To further examine the cytotoxic properties, cell viability was evaluated by MTT assay. A1 cells were cultured in the presence of increasing concentrations of Aβ$_{1-42}$ or ZnPc(COONa)$_8$ for 48 h, and MTT assay was conducted. Aβ$_{1-42}$ dose-dependently decreased the viability of A1 cells, whereas ZnPc(COONa)$_8$ did not (figure 8C). However, when A1 cells were cultured with 5 μM Aβ$_{1-42}$, ZnPc(COONa)$_8$ partially rescued the cells from Aβ$_{1-42}$-induced cytotoxicity in a dose-dependent manner (figure 8D).

Discussion:

Our present results indicate that a water-soluble Zn-phthalocyanine, $ZnPc(COONa)_8$, binds to Aβ peptide and inhibits aggregation, apparently by altering the microenvironment of fibril formation. This is important, because Aβ aggregation and deposition play a vital role in the pathogenesis of AD and could be useful as a disease marker [2]. Since $ZnPc(COONa)_8$ shows near-infrared optical properties, it may have potential as a diagnostic imaging probe for AD, in addition to being a candidate therapeutic agent.

The inhibitory effects on Aβ fibril formation were both dose-dependent and dependent on the species of phthalocyanine. In a report, it has been shown that tetrasulfonated phthalocyanines interact with α-synuclein during the fibril formation process in a manner that depends on the nature of the metal at the macrocyclic center [18], and that iron-containing phthalocyanine promoted conversion of $Aβ_{1-40}$ oligomer to a fibril meshwork [19]. In the present work, the two carboxylated Pcs were water-soluble, while $ZnPc(COOC_5H_{11})_8$ and PdPc dimer were not, and since only the carboxylated Pcs inhibited Aβ fibril formation, the differential interaction with Aβ may reflect the differences in hydrophilicity of the compounds. Interestingly, $ZnPc(COONa)_8$ showed a much stronger

inhibitory effect than $ZnPc(COONa)_{16}$ despite having similar solubility, so structural differences also appear to be important. In addition, $ZnPc(COONa)_8$ had a much greater inhibitory effect on $A\beta_{1-40}$ than on $A\beta_{1-42}$ fibril formation. Fibril formation of both $A\beta_{1-40}$ and $A\beta_{1-42}$ is a nucleation-dependent process, in which the surfactant properties of the peptide, provided by the hydrophobic amino acids at the C-terminus play a pivotal role [31]. $A\beta_{1-42}$ polymerizes much faster than $A\beta_{1-40}$ because of the presence of two more hydrophobic amino acids at the C-terminus [32], and this might also account at least in part for the differential interaction of $ZnPc(COONa)_8$ with the peptides.

$ZnPc(COONa)_8$ not only inhibited Aβ fibril formation process, but also destabilized pre-formed fibrils. Fibril formation is a dynamic process, in which association of the monomers to polymers, and dissociation of the polymers to monomer and other low-molecular-weight species occur side by side. Initially, the concentrations of monomer and other low-molecular-weight species are high. As a result, the rate of association is greater than that of dissociation, while at the plateau stage, the rates of association and dissociation are in equilibrium [33]. Our binding assay showed that $ZnPc(COONa)_8$ had a higher binding ability to monomers and other low-molecular-weight species than to preformed Aβ

fibrils. Therefore, in the destabilization experiment, the monomer and low-molecular-weight species of Aβ might preferentially bind to $ZnPc(COONa)_8$ after dissociation from the fibrils, disturbing the fibril formation equilibrium. We confirmed that addition of $ZnPc(COONa)_8$ to fibrils increases the amount of low-molecular-weight species, at least in the case of $Aβ_{1-40}$.

Pthalocyanines are known to produce singlet oxygen in the presence of light [23], and singlet oxygen interacts with various biomolecules, including proteins. Therefore, we investigated whether singlet oxygen has a role in the inhibition of fibril formation. However, sodium azide, a scavenger of singlet oxygen [24], did not influence the inhibitory effect of $ZnPc(COONa)_8$, suggesting that singlet oxygen plays no role in the process.

We found that ZnPc binds to Aβ peptide during fibril formation, and this binding may play a role in the inhibition of fibril formation. Compounds having aromatic ring structure can interact with amyloid-forming peptides [34, 35], but non-inhibitory phthalocyanines such as $ZnPc(COOC_5H_{11})_8$ also contain aromatic rings. Since the inhibitory effect was specific to $ZnPc(COONa)_8$ and $ZnPc(COONa)_{16}$, other parts of the compound besides the aromatic rings, such as the sodium carboxylated side chains, could be more important for the

interaction. Zinc ion can interact with Aβ peptide and modulate fibril formation (36, 37), but the differential effects of $ZnPc(COONa)_8$ and $ZnPc(COONa)_{16}$ on Aβ fibril formation suggest that it is not a major factor. We consider that the presence and amount of sodium carboxylate groups in ZnPc are important for the interaction with Aβ peptide.

The nucleation-dependent Aβ aggregation process involves hydrophobic interaction of the C-terminal hydrophobic amino acids in an aqueous environment [29, 30]. ANS, a hydrophobic fluorescent dye, is widely used to probe protein conformational changes, since its fluorescence dramatically increases in a hydrophobic environment [28]. We found that addition of $ZnPc(COONa)_8$ caused an early and sustained reduction of ANS fluorescence. Since different molecular species, such as oligomers, prefibrillar aggregates and mature fibrils, might have different binding affinity to ANS, the change in the ANS fluorescence might reflect changes in the proportions of the different molecular species of Aβ caused by the binding of $ZnPc(COONa)_8$. The β-sheet population of Aβ, which is affected by hydrophobic environment [25], was observed to be decreased by $ZnPc(COONa)_8$ from an early time point during fibril formation. We found that Aβ monomer, dimer, trimer and tetramer decreased with time, while

larger oligomers increased during fibril formation. But, in the presence of $ZnPc(COONa)_8$, the reduction of low-molecular-weight species and the appearance of oligomers were delayed. Taken together, our results suggest that $ZnPc(COONa)_8$ alters the fibril-formation microenvironment, thereby inhibiting nucleation and oligomerization.

Finally, we examined the effect of ZnPc on neuronal viability. In agreement with previous studies [38], our preliminary experiments showed that $ZnPc(COONa)_8$ was accumulated inside the cells in a neuronal cell culture system (data not shown). Nevertheless, $ZnPc(COONa)_8$ alone did not decrease the cell viability; rather it provided at least some protection against Aβ-induced neurotoxicity. Aβ oligomers are considered to be the most toxic species of Aβ [11, 12]. Thus, the decrease of oligomer formation by $ZnPc(COONa)_8$ might account for the neuroprotective effect.

In conclusion, our results indicate that water-soluble $ZnPc(COONa)_8$ binds to Aβ peptides and inhibits the oligomerization and subsequent fibril formation processes. It also destabilizes pre-formed fibrils. We consider that $ZnPc(COONa)_8$ has potential value as a diagnostic probe for near-infrared imaging of fibrils in AD brains, and it may also be a candidate for therapy of AD.

Materials and Methods

Materials

$A\beta_{1-40}$ and $A\beta_{1-42}$ were purchased from Peptide Institute, Osaka, Japan. The peptides were dissolved in 0.1% NH_3 at a concentration of 250 μM, immediately aliquoted, and stored at -70°C. Chromatographic data provided by the manufacturer indicated monomeric purity of the peptides. Thioflavin T (ThT) and filter-sterilized deionized water were purchased from Wako Pure Chemicals (Richmond, VA, USA) and Sigma-Aldrich (St Louis, MO, USA), respectively. Prestained protein size markers were from Nippon Genetics Europe GmbH (Duren, Germany), and 4-20% Tris-glycine polyacrylamide from Bio-Rad (Hercules, CA, USA). Nitrocellulose membrane for dot blot assay was obtained from Millipore (Billerica, MA, USA).

Synthesis of Phthalocyanines

In this study, 4 phthalocyanines were used. $ZnPc(COONa)_8$ and $ZnPc(COONa)_{16}$ were dissolved in H_2O. $ZnPc(COOC_5H_{11})_8$ and PdPc dimer were dissolved in chloroform. The phthalocyanines were each dissolved at 1 mM concentration and the solutions were stored at -20°C until use. Preparation of

these phthalocyanines [39, 40] is described below.

$ZnPc(COOC_5H_{11})_8$:

A mixture of 4,5-dichlorophthalonitrile (1.0 g, 5.1 mmol) and *n*-hexyl-4-hydroxylbenzoate (4.3 g, 19.3 mmol) in DMF (60 ml) was stirred in the presence of K_2CO_3 (4 × 4 g) at 65 °C for 24 h. The reaction mixture was poured into ice-cold water to give a white-brown precipitate, which was extracted with $CHCl_3$ (5 × 100 ml). The organic extracts were dried over anhydrous $MgSO_4$ (25 g) and concentrated under vacuum to give a yellow oil. Recrystallization from methanol gave 4, 5-bis[(4-hexyloxycarbonyl)phenoxy]phthalonitrile as a white solid (yield: 2.2 g). The obtained compound (460 mg, 0.81 mmol) was employed for the reaction with $Zn(OAc)_2$•2H_2O (65 mg, 0.30 mmol) in *n*-pentanol (10 ml) containing a few drops of 1, 8-diazabicyclo[5.4.0]undec-7-ene (DBU). The reaction mixture was refluxed overnight, and then volatiles were removed under reduced pressure to give a greenish-blue solid. During the nitrile cyclization reaction in *n*-pentanol, hexyloxy groups on the nitrile were replaced with pentoxy groups from the reaction solvent. Recrystallization of the crude product from EtOH/H_2O gave the title complex $ZnPc(COOC_5H_{11})_8$ as a green solid (yield: 280 mg).

$ZnPc(COONa)_{16}$:

A mixture of 4,5-dichlorophthalonitrile**,** 5-hydroxyisophthalate, and K_2CO_3 in DMF was stirred at 65 °C for 24 h, and then poured into ice-cold water to give a white-brown precipitate, which was extracted with $CHCl_3$. The organic extracts were dried over anhydrous $MgSO_4$ and concentrated under vacuum to give a yellow oil. Recrystallization from methanol afforded 4,

5-bis[(3,5-bismethoxycarbonyl)phenoxy]phthalonitrile (1st compound) as a white solid.

The 1st compound was mixed with $Zn(OAc)_2 \cdot 2H_2O$ and a few drops of 1,8-diazabicyclo[5.4.0]undec-7-ene (DBU) in *n*-pentanol, and refluxed overnight. The volatiles were removed under vacuum to give a greenish-blue solid, which was purified by column chromatography with dichloromethane/ethyl acetate (20:1). The crude product was recrystallized from THF/MeOH to give the 2nd compound zinc(II) 2,3,9,10,16,17,23,24-octakis[(3',5'-bispentyloxycarbonyl)phenoxy]phthalocyanine as a green solid.

The 2nd compound was dissolved in THF and the solution was added slowly to a saturated NaOH solution in water/methanol (1:5) (100 ml). The mixture was stirred at 40°C for 4 h. The resulting precipitate was collected by filtration, washed repeatedly with MeOH and $CHCl_3$, dissolved in water, and neutralized with 1 M HCl (to pH 7). The title compound $ZnPc(COONa)_{16}$ was precipitated as a green solid upon addition of ethanol.

$ZnPc(COONa)_8$:

Saturated NaOH solution in water/methanol (1:5) (100 ml) was added slowly to a THF (5 ml) solution of $ZnPc(COOC_5H_{11})_8$ (200 mg). The mixture was stirred at 40°C for 4 h. The resulting precipitate was collected by filtration, washed repeatedly with MeOH and $CHCl_3$, dissolved in water and neutralized with 1 M HCl (to pH 7). Ethanol was added to precipitate $ZnPc(COONa)_8$ as a green solid (yield: 66 mg).

PdPc Dimer:

A mixture of 4,5-bis(2,6-dimethylphenoxy)phthalonitrile (997 mg, 2.7 mmol), bis(1,3-diiminoisoindoline) (115 mg, 0.54 mmol), and $PdCl_2$ (295 mg, 1.7 mmol) in *n*-propanol (10 ml) and 1,8-diazabicyclo[5.4.0]undec-7-ene (DBU) (1.0 ml) was heated at 110°C for 30 h. After the reaction mixture had cooled, toluene (30 ml) was added and the resulting precipitate was collected by filtration, and vacuum-dried to give a green solid. This product was dissolved in toluene and subjected to GPC chromatography with toluene as an eluent to afford two major fractions. PdPc dimer was obtained from the first fraction (yield: 112 mg) and PcPc from the second fraction (yield: 645 mg).

Aβ fibril formation

Synthetic Aβ peptides were added to fibril-forming buffer [50 mM phosphate buffer (pH 7.5) and 100 mM NaCl] containing various concentrations of phthalocyanines [41]. As a control, peptides were added to fibril-forming buffer without phthalocyanines (addition of solvent only). The reaction mixtures were incubated for the indicated times at 37^{o}C without agitation, and then the reaction was terminated by freezing the samples quickly.

Quantitation of Aβ fibril formation

Aβ fibril formation was determined by ThT fluorescence spectroscopy [41]. Samples were diluted tenfold with glycine (pH 8.5, 50 mM final

concentration), then ThT was added (5 μM final concentration), and the fluorescence was measured with excitation at 446 and emission at 490 nm using a fluorescence spectrophotometer (F2500 spectrofluorimeter, Hitachi, Tokyo, Japan). The florescence intensity of Aβ fibrils in a sample was normalized by subtracting the florescence intensity of the buffer alone.

For further evaluation of fibril formation, 25 μg $A\beta_{1-42}$ at 100 μM concentration in the absence or presence of $ZnPc(COONa)_8$ (5 μM) was used for fibril formation for 24 h. The fibrils were removed from the samples using a 100 KDa cut-off filter (Amicon, Millipore, Tulagreen, Ireland), and the filtrates were concentrated by evaporation. Total protein in the filtrates was measured with a UV/Vis spectrophotometer (ND-1000, NanoDrop Technologies, Wilmington, DE, USA) in terms of absorbance at 280 nm.

Electron microscopic analysis of Aβ fibrils

Electron microscopic analysis of Aβ fibrils were done as described previously [41]. Briefly, after incubation of Aβ (50 μM) in the absence or presence of $ZnPc(COONa)_8$ (5 μM) for desired times, the sample (5 μl) was applied to a carbon-coated Formvar grid (Nisshin EM, Tokyo, Japan). After incubation for 1 min, an equal volume of 0.5% v/v glutaraldehyde solution was

applied to displace the sample, and incubation was continued for an additional 1 min. The grid was washed with water and dried. Then 10 µl of 2% w⁄v uranyl acetate solution was applied and the grid was incubated for 2 min. Finally, uranyl acetate was soaked off, and the grid was air-dried and examined under an electron microscope (EM-002B, Topcon, Tokyo, Japan).

ANS fluorescence assay

To analyze the relative exposure of hydrophobic surfaces of $A\beta_{1-42}$, we measured the change of 8-anilino-1-naphthalenesulfonic acid (ANS) (Sigma, St. Lois, MO, USA) fluorescence intensity, using a Hitachi F2500 spectrofluorimeter. The excitation wavelength was 360, and emission was scanned from 380 to 600 nm at a rate of 300 nm/min. Slit widths for excitation and emission were 5 nm. Maximum emission is presented as the mean ± SEM of three independent experiments, and is expressed in arbitrary fluorescence units.

Gel electrophoresis analysis of Aβ

After fibril formation, Aβ samples were separated by SDS PAGE using 4–20% gradient tris-glycine gel (Biorad). For electrophoresis, 2x SDS non-reducing sample buffer (Invitrogen, Carlsbad, CA, USA) was added to 2 µg of Aβ peptide in a final volume of 20 µl, and the mixture was incubated for 2 min

at 85°C. After electrophoresis, the gel was fixed with fixation buffer (40% methanol and 10% acetic acid) for 30 min, and then stained for 1 h with Coomassie Blue G250 (Biosafe Coomassie; Bio-Rad). After staining, the gel was washed overnight with water, and scanned using a gel scanner (Bio-Rad).

Determination of oligomers by dot-blot immunoassay

After fibril formation, aliquots equivalent to 2 μg of $A\beta_{1-42}$ peptide were spotted on a nitrocellulose membrane. To detect oligomer, an oligomer-specific antibody (A11, Invitrogen) was used; this antibody specifically reacts with a variety of soluble oligomeric protein/peptide aggregates including Aβ, regardless of their amino acid sequence, and does not react with monomer species or insoluble fibrils of protein/peptide [42]. In the case of Aβ oligomer, it has been shown to react with species of at least octamer in size. To detect immunoreactive oligomer, an infrared dye-conjugated anti-rabbit IgG and Odessey infrared dye scanning system (Li-Cor Biosciences, Lincoln, NE, USA) were used according to the manufacturer's instructions.

Phthalocyanine binding assay

To determine the binding of $ZnPc(COONa)_8$ with Aβ peptide, $A\beta_{1-42}$ (50 μM) and the indicated concentrations of $ZnPc(COONa)_8$ were incubated in

fibril-forming buffer for 24 h. To evaluate the binding with the fibrils, Aβ fibrils were prepared by incubation of the peptide in fibril-forming buffer for 24 h, then the indicated concentrations of $ZnPc(COONa)_8$ were added to the fibril to make the concentration of the peptide to 50 μM, and incubation was continued for 24 h. Five micrograms of peptide was immunoprecipitated with a monoclonal anti-Aβ specific antibody (Santa Cruz, Dallas, Tx, USA). The immunoprecipitates were placed on a ELISA plate and scanned at 680 nm using an Odessey infrared scanner (Li-Cor) to detect $ZnPc(COONa)_8$. Two negative controls were run: fibril-forming buffer alone containing the indicated concentrations of $ZnPc(COONa)_8$ was immunoprecipitated with anti-Aβ specific antibody, and mouse normal IgG was used for immunoprecipitation instead of anti-Aβ specific antibody.

Analysis of secondary structures of Aβ peptide

To prepare samples for evaluation of changes of secondary structures during fibril formation, $ZnPc(COONa)_8$ (2 μM) was added to $Aβ_{1-40}$ (100 μM) monomers in fibril-forming buffer, and the mixture was incubated at 37°C for 0 and 2 h. The samples were diluted with water to make final concentrations of $Aβ_{1-40}$ and $ZnPc(COONa)_8$ of 10 μM and 0.2 μM, respectively. Then the circular dichroism (CD) spectra in the range of 190 – 250 nm were acquired at 50 nm/min using a Jasco J-720 spectropolarimeter (Jasco Corporation, Tokyo,

Japan) and a quartz cell with 3 mm optical path length. The results were expressed as mean residue molar ellipticity, and the percentages of secondary structures in the samples were estimated with the Protein Secondary Structure Estimation Program (Jasco Corp.) using published reference CD spectra [43].

Cell culture

Human neuronal cell line A1 was generated by somatic fusion between a human fetal cerebral neuron and a human neuroblastoma cell, and shows characteristic morphological, electrophysiological and expressional features of neurons [44]. A1 cells were cultured in 5% FBS (Gibco) containing DMEM medium (Wako). During stimulation with $A\beta_{1-42}$ and $ZnPc(COONa)_8$, the concentration of FBS was reduced to 1%. Photomicrographs of the cultured cells were obtained with an inverted cell culture microscope equipped with a digital photography system.

MTT cell viability assay

The effect of $ZnPc(COONa)_8$ on Aβ-induced neuronal toxicity was evaluated by MTT cell viability assay, as described previously [45]. Briefly, A1 cells ($3X10^3$/well) were seeded on wells of a 96-well plate and cultured for 48 h. The cells were treated with the indicated concentrations of $ZnPc(COONa)_8$, $A\beta_{1-42}$ or both $A\beta_{1-42}$ and $ZnPc(COONa)_8$ in 100 μl of 1% FBS containing DMEM

for 48 h. After incubation, 20 µl of MTT solution (Sigma) (5 mg/ml) was added to the culture medium and incubation was continued for 3.5 h at 37^{o}C. Then the medium was removed carefully, MTT solvent (4 mM HCl, 0.1% Nondet P-40 in isopropanol) was added, and incubation was continued for 15 min at room temperature with protection from light. The absorbance was read at 590 nm. The absorbance of the cells under normal culture conditions was used as a control.

Statistical analysis

The results are expressed as mean ± SEM of at least three independent experiments. Statistical analysis for comparing mean values was performed using one-way ANOVA, followed by Scheffe's post hoc test, or *student's t* test. Fibril formation kinetics were analyzed using SigmaPlot software (Systat Software Inc, San Jose, CA, USA), and p values < 0.05 were taken as indicating statistical significance.

Acknowledgement: This study was supported by JSPS KAKENHI Grant Number 24310102.

Author contributions. ST planned and performed the experiments, analyzed

the data and prepared the manuscript. AS planned the experiments, analyzed the data and prepared the manuscript. SY analyzed the data and prepared the manuscript. MH prepared phthalocyanines, analyzed the data and prepared the manuscript. TI prepared phthalocyanines, analyzed the data and prepared the manuscript. AN planned the experiments, provided the reagents and other essential materials, prepared the manuscript, and supervised the overall study.

References:

1. Rowland LP, Pedley TA & Merritt HH (2010) *Merritt's Neurology*, 12 edn. pp. 713- 717. Lippincott Williams & Wilkins. Philadelphia, PA

2. Duyckaerts C, Delatour B, & Potier MC (2009) Classification and basic pathology of Alzheimer disease. *Acta Neuropathol* **118**, 5-36.

3. Francis PT, Palmer AM, Snape M & Wilcock GK (1999) The cholinergic hypothesis of Alzheimer's disease: a review of progress. *J Neurol Neurosurg Psychiatry* **66**, 137– 147

4. Campion D, Flaman JM, Brice A, Hannequin D, Dubois B, Martin C, Moreau V, Charbonnier F, Didierjean O, Tardieu S & et al. (1995) Mutations of the presenilin I gene in families with early-onset Alzheimer's disease. *Hum Mol Genet* **4**, 2373-2377.

5. Goate A, Chartier-Harlin MC, Mullan M, Brown J, Crawford F, Fidani L, Giuffra L, Haynes A, Irving N, James L & et al. (1991) Segregation of a missense

mutation in the amyloid precursor protein gene with familial Alzheimer's disease. *Nature* **349**, 704-706.

6. Hardy J & Selkoe DJ (2002) The amyloid hypothesis of Alzheimer's disease: progress and problems on the road to therapeutics. *Science* **297**, 353-356.

7. Richards SJ, Waters JJ, Beyreuther K, Masters CL, Wischik CM, Sparkman DR, White CL 3rd, Abraham CR & Dunnett SB (1991) Transplants of mouse trisomy 16 hippocampus provide a model of Alzheimer's disease neuropathology. *EMBO J* **10**, 297-303.

8. Sisodia SS, Kim SH & Thinakaran G (1999) Function and dysfunction of the presenilins. *Am J Hum Genet* **65**, 7-12.

9. Xia W, Zhang J, Kholodenko D, Citron M, Podlisny MB, Teplow DB, Haass C, Seubert P, Koo EH & Selkoe DJ (1997) Enhanced production and oligomerization of the 42-residue amyloid beta-protein by Chinese hamster ovary cells stably expressing mutant presenilins. *J Biol Chem* **272**, 7977-7982.

10. Yoshioka K, Miki T, Katsuya T, Ogihara T & Sakaki Y (1991) The 717Val----Ile substitution in amyloid precursor protein is associated with familial Alzheimer's disease regardless of ethnic groups. *Biochem Biophys Res Commun* **178**, 1141-1146.

11. Cotman CW, Whittemore ER, Watt JA, Anderson AJ & Loo DT (1994) Possible role of apoptosis in Alzheimer's disease. *Ann N Y Acad Sci* **747**, 36-49.

12. Malaplate-Armand C, Florent-Béchard S, Youssef I, Koziel V, Sponne I, Kriem B, Leininger-Muller B, Olivier JL, Oster T & Pillot T (2006) Soluble oligomers of amyloid-beta peptide induce neuronal apoptosis by activating a

cPLA2-dependent sphingomyelinase-ceramide pathway. *Neurobiol Dis* **23**, 178-189.

13. Iqbal K, Liu F. & Gong CX (2014) Alzheimer disease therapeutics: Focus on the disease and not just plaques and tangles. *Biochem Pharmacol* **88**, 631-639.

14. Leger GC & Massoud F (2013) Novel disease-modifying therapeutics for the treatment of Alzheimer's disease. *Expert Rev Clin Pharmacol* **6**, 423-442.

15. Cruchaga C, Ebbert MT & Kauwe JS (2014) Genetic discoveries in AD using CSF amyloid and tau. *Curr Genet Med Rep* **2**, 23-29.

16. Petrella JR (2013) Neuroimaging and the search for a cure for Alzheimer disease. *Radiology* **269**, 671-691.

17. Hilderbrand SA & Weissleder R (2010) Near-infrared fluorescence: application to in vivo molecular imaging. *Curr Opin Chem Biol* **14**, 71-79.

18. Lee EN, Cho HJ, Lee CH, Lee D, Chung KC & Paik SR (2004) Phthalocyanine tetrasulfonates affect the amyloid formation and cytotoxicity of alpha-synuclein. *Biochemistry* **43**, 3704-3715.

19. Park JW, Ahn JS, Lee JH, Bhak G, Jung S & Paik SR (2008) Amyloid fibrillar meshwork formation of iron-induced oligomeric species of Abeta40 with phthalocyanine tetrasulfonate and its toxic consequences. *Chembiochem* **9**, 2602-2605.

20. Simon J & Vacus J (1995) Luminescence and anti-aggregative properties of polyoxyethylene-substituted phthalocyanine complexes. *Adv Mater* **7**, 797-800.

21. Spikes JD (1986) Phthalocyanines as photosensitizers in biological systems and for the photodynamic therapy of tumors. *Photochem Photobiol* **43**, 691-699.

22. Moss MA, Varvel NH, Nichols MR, Reed DK & Rosenberry T L (2004)

Nordihydroguaiaretic acid does not disaggregate beta-amyloid(1-40) protofibrils but does inhibit growth arising from direct protofibril association. *Mol Pharmacol* **66**, 592-600.

23. Agarwal R, Athar M, Urban SA, Bickers DR & Mukhtar H (1991) Involvement of singlet oxygen in chloroaluminum phthalocyanine tetrasulfonate-mediated photoenhancement of lipid peroxidation in rat epidermal microsomes. *Cancer Lett* **56**, 125-129.

24. Bancirova M (2011) Sodium azide as a specific quencher of singlet oxygen during chemiluminescent detection by luminol and Cypridina luciferin analogues. *Luminescence* **26**, 685-688.

25. Kowalewski T & Holtzman DM (1999) In situ atomic force microscopy study of Alzheimer's beta-amyloid peptide on different substrates: new insights into mechanism of beta-sheet formation. *Proc Natl Acad Sci U S A* **96**, 3688-3693.

26. Marshall KE, Morris KL, Charlton D, O'Reilly N, Lewis L, Walden H & Serpell LC (2011) Hydrophobic, aromatic, and electrostatic interactions play a central role in amyloid fibril formation and stability. *Biochemistry* **50**, 2061-2071

27. Tjernberg LO, Callaway DJ, Tjernberg A, Hahne S, Lilliehöök C, Terenius L, Thyberg J & Nordstedt C (1999) A molecular model of Alzheimer amyloid beta-peptide fibril formation. *J Biol Chem* **274**, 12619-12625

28. Hawe A, Sutter M & Jiskoot W (2008) Extrinsic fluorescent dyes as tools for protein characterization. *Pharm Res* **25**, 1487-1499.

29. Hills RD Jr & Brooks CL 3rd (2007) Hydrophobic cooperativity as a mechanism for amyloid nucleation. *J Mol Biol* **368**, 894-901.

30. Serpell LC (2000) Alzheimer's amyloid fibrils: structure and assembly.

Biochim Biophys Acta **1502**, 16-30

31. Soreghan B, Kosmoski J & Glabe C (1994) Surfactant properties of Alzheimer's A beta peptides and the mechanism of amyloid aggregation. *J Biol Chem* **269**, 28551-28554.

32. El-Agnaf OM, Mahil DS, Patel BP & Austen BM (2000) Oligomerization and toxicity of beta-amyloid-42 implicated in Alzheimer's disease. *Biochem Biophys Res Commun* **273**, 1003-1007.

33. Morris AM, Watzky MA & Finke RG (2009) Protein aggregation kinetics, mechanism, and curve-fitting: a review of the literature. *Biochim Biophys Acta* **1794**, 375-97.

34. Porat Y, Abramowitz A & Gazit E (2006) Inhibition of amyloid fibril formation by polyphenols: structural similarity and aromatic interactions as a common inhibition mechanism. *Chem Biology Drug Des* **67**, 27-37.

35. McLaughlin RW, De Stigter JK, Sikkink LA, Baden EM & Ramirez-Alvarado M (2006) The effects of sodium sulfate, glycosaminoglycans, and Congo red on the structure, stability, and amyloid formation of an immunoglobulin light-chain protein. *Protein Sci* **15**, 1710-22.

36. Bush AI, Pettingell WH, Multhaup G, d Paradis M, Vonsattel JP, Gusella JF, Beyreuther K, Masters CL & Tanzi RE (1994) Rapid induction of Alzheimer A beta amyloid formation by zinc. *Science* **265**, 1464-1467.

37. Esler WP, Stimson ER, Jennings JM, Ghilardi JR, Mantyh PW & Maggio JE (1996) Zinc-induced aggregation of human and rat beta-amyloid peptides in vitro. *J Neurochem* **66**, 723-732.

38. Trivedi NS, Wang HW, Nieminen AL, Oleinick NL & Izatt JA (2000)

Quantitative analysis of Pc 4 localization in mouse lymphoma (LY-R) cells via double-label confocal fluorescence microscopy. *Photochem Photobiol* **71**, 634-9.

39. Ikeue T, Sonoda M, Kurahashi S, Tachibana H, Teraoka D, Sugimori T, Kasuga K & Handa M (2010) Annulated dinuclear palladium (II) phthalocyanine complex as an effective photo-oxidation catalyst for near-infrared region light. *Inorganic Chemistry Comm.* **13**, 1170-1172.

40. Liu W, Jensen TJ, Fronczek FR, Hammer RP, Smith KM & Vicente MG (2005) Synthesis and cellular studies of nonaggregated water-soluble phthalocyanines. *J Med Chem* **48**, 1033-1041.

41. Sheikh AM & Nagai A (2011) Lysophosphatidylcholine modulates fibril formation of amyloid beta peptide. *FEBS J* **278**, 634-642.

42. Kayed R, Head E, Thompson JL, McIntire TM, Milton SC, Cotman CW & Glabe CG (2003) Common structure of soluble amyloid oligomers implies common mechanism of pathogenesis. *Science* **300**, 486-489.

43. Yang JT, Wu CS, Martinez HM (1986) Calculation of protein conformation from circular dichroism. Methods Enzymol 130, 208-269

44. Nagai A, Suzuki Y, Baek SY, Lee KS, Lee MC, McLarnon JG & Kim SU (2002) Generation and characterization of human hybrid neurons produced between embryonic CNS neurons and neuroblastoma cells. *Neurobiol Dis* **11**, 184-198.

45. Nagai A, Ryu JK, Terashima M, Tanigawa Y, Wakabayashi K, McLarnon JG, Kobayashi S, Masuda J & Kim SU 2005. Neuronal cell death induced by cystatin C in vivo and in cultured human CNS neurons is inhibited with cathepsin B. *Brain Res* **1066**, 120-128.

Figure legends

Figure 1: **Structures of phthalocyanines used in the experiments.** The chemical structures of $ZnPc(COONa)_8$ (A), $ZnPc(COONa)_{16}$ (B), $ZnPc(OOC_5H_{11})_8$ (C) and Pd-Pc dimer (D) are shown.

Figure 2: Effect of phthalocyanines on Aβ peptide fibril formation. $A\beta_{1-40}$ (50 μM) (A, C, E and G) or $A\beta_{1-42}$ (12.5 μM) (B, D, F and H) peptide was incubated in fibril-forming buffer for 48 h and 24 h, respectively, in the presence of the indicated concentrations of $ZnPc(COONa)_8$ (A and B), $ZnPc(COONa)_{16}$ (C and D), $ZnPc(COOC_5H_{11})_8$ (E and F) and PdPc dimer (G and H). Total fibril formation at the end of incubation was evaluated by ThT fluorescence assay, as described in Materials and Methods. Data shown here are the averages ± SEM of at least 3 independent experiments, and are presented as percent of the Aβ peptide alone (control) condition. $^{*}p<0.05$, $^{‡}p<0.01$ and $^{†}p<0.001$ vs

corresponding 0.1 μM phthalocyanine condition.

Figure 3: Effects of ZnPc(COONa)$_8$ on the fibril formation kinetics of Aβ peptides. Aβ$_{1-40}$ (50 μM) (A and C) or Aβ$_{1-42}$ (12.5 μM) (B and D) peptide was incubated in fibril-forming buffer in the absence (A and B) or presence of ZnPc(COONa)$_8$ (5 μM) (C and D) for the indicated time. Total fibril formation at the end of incubation was evaluated by ThT fluorescence assay, as described in Materials and Methods. Data shown here are the averages ± SEM of ThT fluorescence values (arbitrary unit) of at least 3 independent experiments. The morphology of Aβ fibrils is shown in (E). Aβ$_{1-40}$ (a and c) and Aβ$_{1-42}$ (b and d) peptides (50 μM) were incubated alone (a and b) or with ZnPc(COONa)$_8$ (5 μM) (c and d) for 72 h and 24 h, respectively. Fibril morphology was evaluated by transmission electron microscopy as described in Materials and Methods. Bar = 200 nm. (F) Aβ$_{1-42}$ (100 μM) was incubated alone or with ZnPc(COONa)$_8$ (5 μM) for 24 h. Aliquots of the samples were used for ThT fluorescence assay (left bar). From the remaining samples, fibrils were removed by filtration, and protein in the filtrates (right bar) was measured with an UV/Vis spectrophotometer at 280 nm, as described in Materials and Methods. The data presented here are average ±

SEM of 3 independent experiments, and are expressed as percent of the $A\beta_{1-42}$ peptide alone (control) condition.

Figure 4. Effect of $ZnPc(COONa)_8$ on Aβ fibrils stability. To prepare fibrils, $A\beta_{1-40}$ (50 μM) and $A\beta_{1-42}$ (25 μM) peptides were incubated in fibril-forming buffer for 48 h and 24 h, respectively. The indicated concentrations of $ZnPc(COONa)_8$ were added (final concentration of peptide: 25 μM and 12.5 μM, respectively), and incubation was continued for 24 h. Total fibrils of $A\beta_{1-40}$ (A) and $A\beta_{1-42}$ (B) was evaluated by ThT fluorescence assay. The data are the averages ± SEM of ThT fluorescence values (arbitrary unit) of at least 3 experiments. (C and D) $A\beta_{1-40}$ or $A\beta_{1-42}$ was incubated for 48 and 24 h, respectively. Then, the indicated concentrations of $ZnPc(COONa)_8$ were added to the fibrils (final concentration of peptide: 25 μM). Two micrograms of peptide fibrils were separated using 4-20% gradient Tris-Glycine SDS-PAGE, and the peptide bands of $A\beta_{1-40}$ (C) and $A\beta_{1-42}$ (D) were visualized by Coomassie brilliant blue staining, as described in Materials and Methods. $^{*}p<0.05$, $^{‡}p<0.01$ and $^{†}p<0.001$ vs the corresponding $ZnPc(COONa)_8$ 0 μM condition.

Figure 5. Effect of sodium azide (NaN_3) on $ZnPc(COONa)_8$-mediated inhibition of Aβ fibril formation. The indicated concentration of NaN_3 was added to $Aβ_{1-40}$ (50 μM) (A) and $Aβ_{1-42}$ (12.5 μM) (B) and the mixtures were incubated for 48 h and 24 h, respectively. To evaluate the effects of NaN_3 on $ZnPc(COONa)_8$-mediated inhibition of $Aβ_{1-40}$, and $Aβ_{1-42}$ fibril formation, the indicated concentrations of NaN_3 were added to $Aβ_{1-40}$ (50 μM) (C) and $Aβ_{1-42}$ (12.5 μM) (D) in the presence of $ZnPc(COONa)_8$ (5 μM), and the mixtures were incubated for 48 h and 24 h, respectively. The amount of fibrils formed after incubation was evaluated by ThT fluorescence assay. Data showed here are the average ± SEM of at least 3 experiments, and are presented as percent of the Aβ peptide alone (control) condition.

Figure 6. Binding of $ZnPc(COONa)_8$ to $Aβ_{1-42}$ and change in the hydrophobicity of the fibril-forming microenvironment. (A) $Aβ_{1-42}$ monomer (50 μM) was incubated in fibril-forming buffer with the indicated concentrations of $ZnPc(COONa)_8$ for 24 h. To evaluate the binding ability to preformed fibrils, $Aβ_{1-42}$ fibrils were prepared by incubating the monomer in fibril-forming buffer for 24 h, then the indicated concentration of $ZnPc(COONa)_8$ was added to the fibrils

to give a final concentration of 50 μM, and incubation was continued for 24 h. After incubation, 5 μg of peptide fibrils was used for immunoprecipitation with a monoclonal anti-Aβ IgG. For negative controls, normal mouse IgG, was used instead of anti-Aβ IgG, or buffer containing only $ZnPc(COONa)_8$ was used (without $Aβ_{1-42}$). (B-D) To evaluate the hydrophobic microenvironment, $Aβ_{1-42}$ (12.5 μM) was incubated in the absence or presence of $ZnPc(COONa)_8$ (5 μM) for the indicated time, and ANS fluorescence assay was conducted as described in Materials and Methods. Representative ANS fluorescence emission spectra of $Aβ_{1-42}$ in the absence or presence of $ZnPc(COONa)_8$ at indicated times are shown in (B). The average values of ANS fluorescence intensities (arbitrary unit) and the positions of fluorescence emission maxima (nm) are shown in (C) and (D), respectively. $^{*}p<0.05$ and $^{†}p<0.01$ vs corresponding 0 h condition; $^{\#}p<0.05$ and $^{‡}p<0.01$ vs $Aβ_{1-42}$ condition at the same time point.

Figure 7. Effects of $ZnPc(COONa)_8$ on secondary structure and the oligomerization of Aβ peptide. $Aβ_{1-40}$ (100 μM) was incubated in fibril-forming buffer in the absence or presence of $ZnPc(COONa)_8$ (2 μM) for the indicated time. The samples were then diluted with H_2O to give $Aβ_{1-40}$ and $ZnPc(COONa)_8$

concentrations of 10 and 0.2 μM, respectively, and the changes in secondary structure were evaluated by CD spectroscopy. Representative CD spectra of $A\beta_{1-40}$ alone or $A\beta_{1-40}$ with $ZnPc(COONa)_8$ incubated for 0 and 2 h are shown in (A). The percentage of different secondary structures in a representative experiment is shown in (B). (C) $A\beta_{1-42}$ (50 μM) was incubated in fibril-forming buffer in the absence or presence of $ZnPc(COONa)_8$ (5 μM) for the indicated time. Two micrograms of peptide was separated by 4-20% gradient Tris-glycine SDS-PAGE, and the peptide bands of $A\beta_{1-42}$ species were visualized by Coomassie brilliant blue staining, as described in Materials and Methods. (D) After incubation, 2 μg of peptide was spotted on a nitrocellulose membrane, and $A\beta_{1-42}$ oligomers were detected with oligomer-specific antibody, as described in Materials and Methods.

Figure 8. Effects of $ZnPc(COONa)_8$ on neuronal viability in culture. Cells of a neuronal cell line (A1) were cultured in DMEM medium containing 1% FBS in the presence of the indicated concentrations of $ZnPc(COONa)_8$ or $A\beta_{1-42}$ for 48 h. Representative photomicrographs of A1 cells cultured with $ZnPc(COONa)_8$ (upper row) or $A\beta_{1-42}$ (lower row) are shown in (A). A1 cells were treated with

$A\beta_{1-42}$ (5 μM) and the indicated concentrations of $ZnPc(COONa)_8$. Representative photomicrographs after 48 h treatment are shown in (B). (C) After treatment with the indicated concentrations of $A\beta_{1-42}$ or $ZnPc(COONa)_8$ for 48 h, the viability of A1 cells were evaluated by MTT assay. Average ± SEM data of 3 experiments are shown in (C), where □ represents $ZnPc(COONa)_8$ and ■ represents $A\beta_{1-42}$. (D) A1 cells were cultured with $A\beta_{1-42}$ (5 μM) and the indicated concentrations of $ZnPc(COONa)_8$ for 48 h, and cell viability was evaluated by MTT assay, as described in Materials and Methods. The data are presented in (C) and (D) as percent of the control (viable cells in normal culture). *$p<0.05$ vs $ZnPc(COONa)_8$ 0 μM condition.

Figure 1

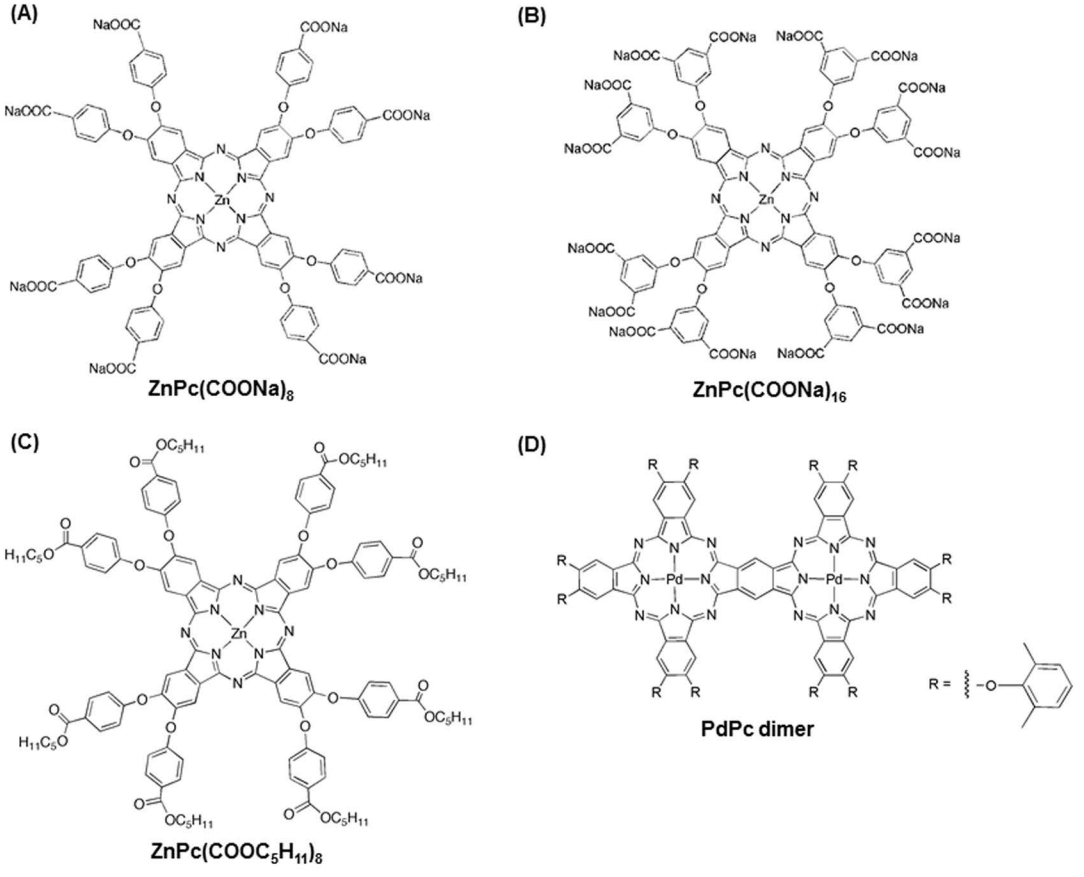
(A)
NaOOC
COONa
Zn
ZnPc(COONa)8
(B)
ZnPc(COONa)16
(C)
OC5H11
H11C5O
ZnPc(COOC5H11)8
(D)
R
Pd
PdPc dimer
R =
O

Figure 2

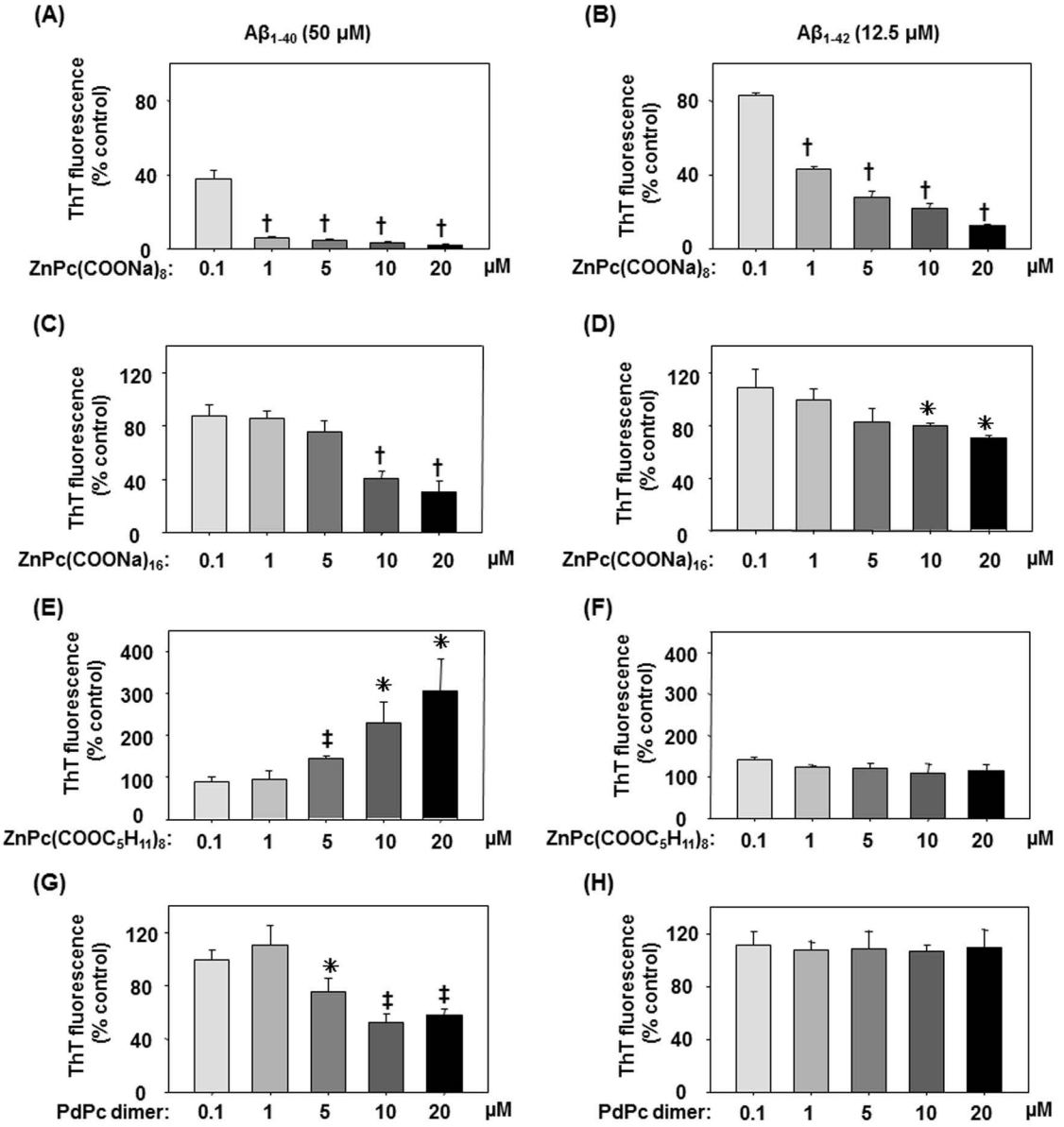
(A)
Aβ1-40 (50 μM)
ThT fluorescence (% control)
ZnPc(COONa)8: 0.1 1 5 10 20 μM
(B)
Aβ1-42 (12.5 μM)
ThT fluorescence (% control)
ZnPc(COONa)8: 0.1 1 5 10 20 μM
(C)
ThT fluorescence (% control)
ZnPc(COONa)16: 0.1 1 5 10 20 μM
(D)
ThT fluorescence (% control)
ZnPc(COONa)16: 0.1 1 5 10 20 μM
(E)
ThT fluorescence (% control)
ZnPc(COOC5H11)8: 0.1 1 5 10 20 μM
(F)
ThT fluorescence (% control)
ZnPc(COOC5H11)8: 0.1 1 5 10 20 μM
(G)
ThT fluorescence (% control)
PdPc dimer: 0.1 1 5 10 20 μM
(H)
ThT fluorescence (% control)
PdPc dimer: 0.1 1 5 10 20 μM